Powder diffraction analysis of gemstone inclusions

Laura Leon-Reina
Servicios Centrales de Investigación, Universidad de Málaga, 29071 Málaga, Spain

José M. Compana and Ángeles G. De la Torre
Departamento de Química Inorgánica, Cristalografía y Mineralogía, Universidad de Málaga, 29071 Málaga, Spain

Rosa Moreno and Luis E. Ochando
Departament de Geologia, Universitat de València, 46100 Burjassot, Valencia, Spain and Instituto de Reconocimiento Molecular y Desarrollo Tecnológico, Campus Burjassot, Valencia, Spain

Miguel A. G. Aranda[a)]
Departamento de Química Inorgánica, Cristalografía y Mineralogía, Universidad de Málaga, 29071 Málaga, Spain

(Received 20 December 2010; accepted 13 January 2011)

Gemstones are pieces of materials that once cut and polished are used as jewels or adornments. Gemstones may be single crystal (such as diamonds), polycrystalline (such as lapis lazuli), or amorphous (such as amber). In any case, gems may have inclusions that may yield a variety of optic effects. It is also important to unravel the crystal structure of the inclusion(s) in order to determine the origin of the gem and to help to understand their formation mechanism. Here, we expand the use of powder diffraction to identify crystalline inclusions in bulk gemstones highlighting Mo $K\alpha$ radiation to penetrate within compact gems. Initially, rock crystal quartz with rutile needles was investigated and rutile diffraction peaks were more conspicuous in the Mo pattern than in the Cu pattern. Next, rock crystal quartz with beetle legs was characterized and the red iron oxide inclusion was identified as hematite. The study of a fake gem, glass showing aventurine effect, gave the diffraction peaks of metallic copper. Later, polycrystalline gems, moss agate, and aventurine quartz were also studied. The powder patterns of these compact gemstones could be successfully fitted using the Rietveld method. Finally, we discuss opportunities for further improvements in laboratory powder diffraction to characterize inclusions in compact gems. © *2011 International Centre for Diffraction Data.* [DOI: 10.1154/1.3552672]

Key words: gemstones, inclusions, X-ray penetration depth, Mo radiation, powder diffraction

I. INTRODUCTION

Broadly defined inclusion is any irregularity observable within a gem by the unaided eye or by using some tools such as a hand lens or a microscope. The "irregularity" may be a crystalline mineral, a fluid filled cavity, an unfilled cavity, a fracture, or even a growth pattern that produces some optical effect. The interested reader is directed to a specialized reference book in order to know about the classification of the types of inclusions and the use of the main instrument, the optical microscope (Gübelin and Koivula, 1986, 2005, 2008). The brief history of research in inclusions may also be of interest (Hughes, 1997).

The study and characterization of inclusions involve some steps, first being to recognize the inclusion(s) by using optical methods: hand lens and/or optical microscope. In the case of crystalline inclusions, a preliminary identification can be carried out based on previous knowledge of (similar) inclusions by analyzing a number of properties under the microscope: color, microcrystal shape, arrangement pattern, mineral host, etc. Although the microscope is the most important tool for inclusion characterization, its use is sometimes not enough for correct inclusion identification. Several techniques are being used for this purpose including laser Raman microspectrometry (Koivula and Chadwick, 2008; Renfro, 2010), electron microprobe analysis (Tagliani *et al.*, 2010), UV irradiation to check the luminescence (Karampelas *et al.*, 2010), cathodoluminiscence (Boiron *et al.*, 1992), and X-ray fluorescence microanalysis. Furthermore, laboratory X-ray powder diffraction (LXRPD) is used for inclusion identification. It is commonly carried out in a micropowder sample obtained by adequate scratching of the gemstones in order to obtain a small amount of powder of the desired inclusion (Gübelin and Koivula, 1986, 2005, 2008). Subsequently, the inclusion is identified by comparison of the obtained powder pattern with those reported in the Powder Diffraction File (PDF) (www.icdd.com). Unfortunately, this "micropowder" methodology is time consuming and destructive. Those who are not familiar with the powder diffraction technique are addressed to some basic publications (Langford and Louër, 1996; Jenkins and Snyder, 1996; Toby, 2007; Pecharsky and Zavalij, 2008).

On the other hand, LXRPD is widely used for characterizing polycrystalline gemstone materials using Cu $K\alpha$ radiation. Generally, selected pieces of the samples are milled and the powders are analyzed for determining the polymorphs, for quantitative phase analysis of the different constituents, or for characterizing the phase microstructure. We underline just a few examples of gemstone materials studied this way:

[a)]Author to whom correspondence should be addressed. Electronic mail: g_aranda@uma.es

opal (Ghisoli *et al.*, 2010), chalcedony (Hatipoglu *et al.*, 2010), pearls (Oaki and Imai, 2005), lapis lazuli (Tarling *et al.*, 1988), etc. Finally, we are aware of the use of Mo $K\alpha$ radiation for the study of the surface of polycrystalline lackluster pearls (Qiao *et al.*, 2007).

Here, we report the use of LXRPD to deeply penetrate within a bulk gemstone by using Mo radiation. So, the inclusions can be characterized without damaging the gem and several examples are reported. Furthermore, we discuss further possible improvements for better inclusion analysis.

II. EXPERIMENTAL

The studied gemstones belong to the didactic gemmology collection of University of Valencia. The optical microphotographs were taken with an Olympus SZX7 stereomicroscope (7 to 70×). This device is equipped with an Olympus SC30 camera, which was PC controlled by CELLÂ software (Version 3.3.).

LXRPD patterns for the gemstones were recorded on a PANalytical X'Pert PRO MPD diffractometer working in reflection geometry ($\theta/2\theta$) and using the X'Celerator real time multiple strip detector with an active length of 2.122°. The gemstones were loaded in a multipurpose holder which allows the micrometric controlled alignment of samples with a mass of up to 1 kg.

Two types of data sets were recorded by using copper and molybdenum radiations. The Cu patterns were collected with a long fine focus Cu tube working at 45 kV and 40 mA. The incident beam optic path contained a hybrid monochromator [composed of a W/Si parabolic X-ray graded mirror and a flat Ge (220) asymmetric monochromator] which yielded a strictly monochromatic, $\lambda = 1.540\,59$ Å, parallel X-ray beam and a fixed 1/8° divergence slit. The diffracted beam optic path contained a fixed 1/8° antiscatter slit. Both incident and diffracted beams were equipped with 0.02 rad Soller slits. A typical scan range was from 5.0 to 80.0°2θ with a step size of 0.0167°2θ and an overall recording time of approximately 4 h.

The Mo patterns were collected by using a long fine focus Mo tube also working at 45 kV and 40 mA. The incident beam optic path contained a 1° fixed antiscatter slit, a 1/4° fixed divergence slit, and a zirconium filter, which resulted in a divergent beam with Mo $K\alpha_{1,2}$ radiations ($\lambda = 0.7093$ and 0.7135 Å). The diffracted beam optic path contained a fixed 1/4° antiscatter slit. A typical scan range was from 2.0 to 35.0°2θ with a step size of 0.0167°2θ and an overall recording time of approximately 1 h. Due to the high penetration of the Mo radiation and in order to avoid (displaced) Al diffraction peaks from the holder, the gemstones were glued to a zero diffraction plate made of single crystal silicon cut at special orientation of 2.0 mm thick.

III. RESULTS AND DISCUSSION

First of all, it must be noted that instead powder diffraction, the technique reported here is better described as X-ray polycrystal diffraction since in this case the samples are bulk compact specimens. This nondestructive methodology can be applied to the main gemstone constituent only if it is polycrystalline (see results for gemstones 608 and 498 below).

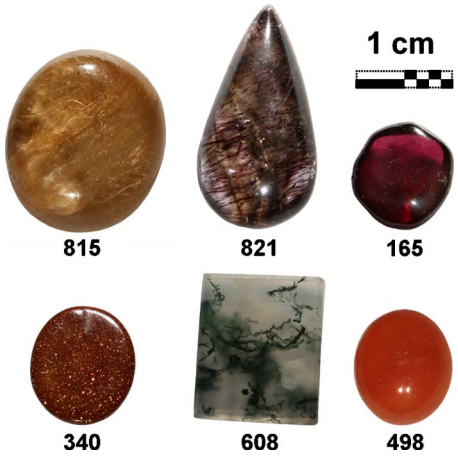

Figure 1. (Color online) Optical photographs of the selected gemstones with their collection codes and scales.

Furthermore, this technique can be applied for characterizing inclusions if they are crystallines. Voids, liquids, and amorphous solid inclusions cannot be studied with this methodology. On the other hand, the amount of inclusion microcrystals does not commonly fulfill the requirement of "randomly arranged infinite number of microparticles" in order to have its recorded XRD data matched the XRD standard data reported in the PDF of ICDD (2004). Therefore, the reported methodology identifies the inclusion from the positions of the XRD peaks and not from their relative intensities. So, the uniqueness of the solution is less ensured than using both positions and relative intensities. However, it should be mentioned that the inclusion phase is not checked against any powder pattern but only against the mineral subset. Furthermore, there are many reports of associations of minerals, which may be used as additional information in case of a doubtful identification.

Second, it should be noted that a high-resolution setup is used for recording the Cu radiation patterns (strictly monochromatic radiation coupled with Soller slits on incident and diffracted beams). This setup significantly reduces the diffracted intensity reaching the detector. This optical configuration has been used to obtain the narrow diffraction peaks and, so, to minimize the overlapping of the reflections. Since there are not enough randomly arranged inclusion crystallites, the values of their relative diffraction intensities cannot be used to identify a given phase as discussed just above. So, the only criterion for identifying a phase is the peak positions, which should be measured as best as possible.

Figure 1 displays the optical photographs of the gemstones selected for this study, and Figure 2 shows the optical microphotographs for these gemstones. The microphotographs highlight the color, shape, and arrangements of the different inclusions within the gemstones.

Gemstone 815 (Figure 1) is a rock crystal quartz with rutile needles. The conclusive identification of the inclusion can be asserted from the optical microphotograph (Figure 2) and there is no need for further inclusion characterization. So, this gem was used as a test example. The Cu and Mo LXRPD patterns for this gem are shown in Figures 3(a) and 3(b), respectively. The diffraction peaks are labeled with the mineral abbreviations adopted within the mineralogy com-

https://doi.org/10.1154/1.3552672 Published online by Cambridge University Press

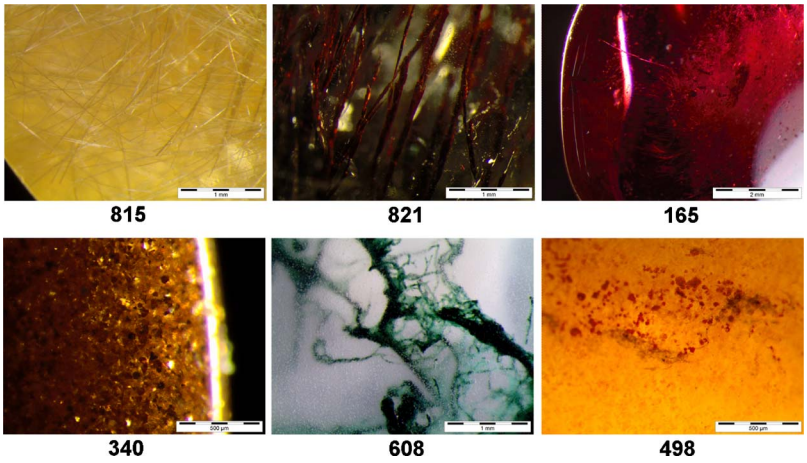

Figure 2. (Color online) Optical microphotographs of the gemstones highlighting the shapes, colors, and arrangements of the inclusions.

munity (Kretz, 1983). The powder patterns are displayed in *d* spacings for the sake of comparison. Three conclusions can be drawn from the diffraction peaks reported in Figures 3(a) and 3(b). First, the peak positions are situated at the expected values from the reported patterns: PDF-01-070-3755 (ICDD, 2004) for quartz and PDF-01-089-4202 (ICDD, 2004) for rutile. Second, the intensities do not match those reported in the PDF database as there are not enough (micro)crystallites diffracting towards the detector direction. Third, and very importantly, the peaks from rutile inclusions are much more evident in the Mo pattern than in the Cu pattern. The higher penetration depth of Mo $K\alpha$ allows irradiating a sample volume containing a larger fraction of rutile inclusions. Therefore, there are more diffraction peaks of rutile and with higher intensities in the Mo pattern. Thus, it is shown that the identification of inclusions deeply buried within a bulk gemstone is easier with Mo radiation, as expected.

Gemstone 821 (Figure 1) is a rock crystal quartz with beetle legs (see Figure 2), where the inclusion is very likely iron oxide. However, to identify the iron oxide phase (usually goethite or hematite) from optical microscopy is not possible. The Cu and Mo LXRPD patterns for this gem are shown in Figures 3(c) and 3(d), respectively. The Cu pattern shows, in addition of a quartz peak, two peaks from hematite (PDF-01-089-8104) (ICDD, 2004) and one likely from goethite (PDF-01-081-0463) (ICDD, 2004). However, the deeply penetrating Mo radiation yielded a pattern with many peaks from hematite and no diffraction peak from goethite. Therefore, it can be concluded that the iron oxide inclusion within this beetle-leg rock crystal is mainly hematite.

Gemstone 165 (Figure 1) is an almandine garnet. The inclusions are deep in the gem (see Figure 2), so a Mo LXRPD pattern was collected. Figure 4(a) shows the pattern where, in addition to the almandine diffraction peaks (PDF-01-089-4372) (ICDD, 2004), only peaks from rutile (PDF-01-089-4202) are evident. Therefore, the needles visible in Figure 2 arise from rutile. Gemstone 340 (Figure 1) is a glass fabricated to display the aventurine effect. This beautiful optical effect was achieved with the platelet microparticles (inclusions) highlighted in Figure 2. Figure 4(b) shows the Mo LXRPD pattern of this gemstone. In addition to a broad band centered approximately at 3.3 Å, due to the glass matrix, the only diffraction peaks are those corresponding to the copper metal inclusion (PDF-01-085-1326) (ICDD, 2004).

Gemstone 608 (Figure 1) is a moss agate. The green inclusions are highlighted in Figure 2. The Cu and Mo LXRPD patterns for this gem are shown in Figures 5(a) and 5(b), respectively. As the main constituent of this gem is polycrystalline quartz, the Rietveld method (Rietveld, 1969) can be applied to characterize the gemstone. This has been carried out by using the GSAS program (Larson and von Dreele, 2000) with the EXPGUI graphic interface (Toby, 2001). First, it can be seen that the diffraction peaks of quartz in the Cu pattern are sharper than in the Mo pattern. This is due to the optical setup that was used, as the Cu

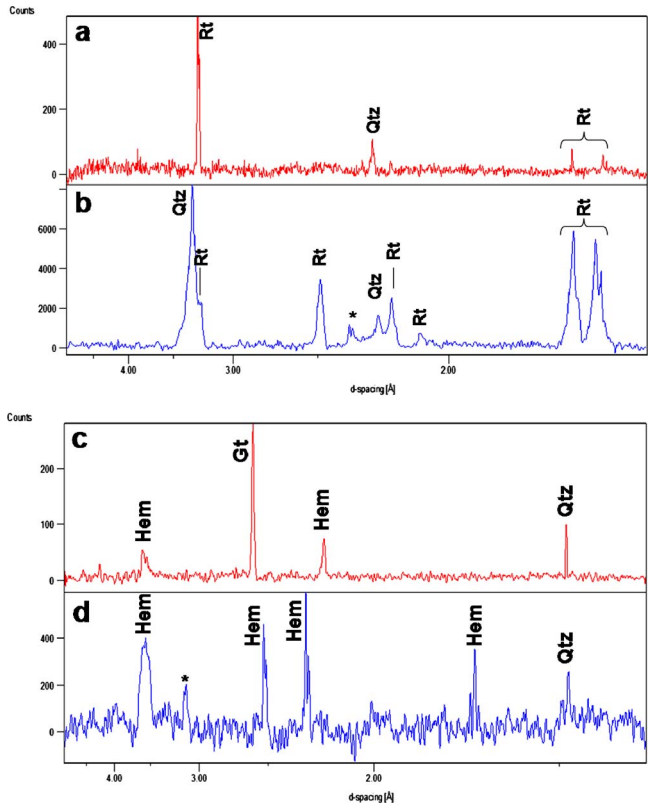

Figure 3. (Color online) LXRPD patterns for (a) gem-815 with Cu radiation ($\lambda = 1.540\,59$ Å), (b) gem-815 with Mo radiations ($\lambda = 0.7093$ and 0.7135 Å), (c) gem-821 with Cu radiation, and (d) gem-821 with Mo radiations. The diffraction peaks are labeled with the corresponding mineral abbreviation and the asterisk highlights unjustified peak(s).

https://doi.org/10.1154/1.3552672 Published online by Cambridge University Press

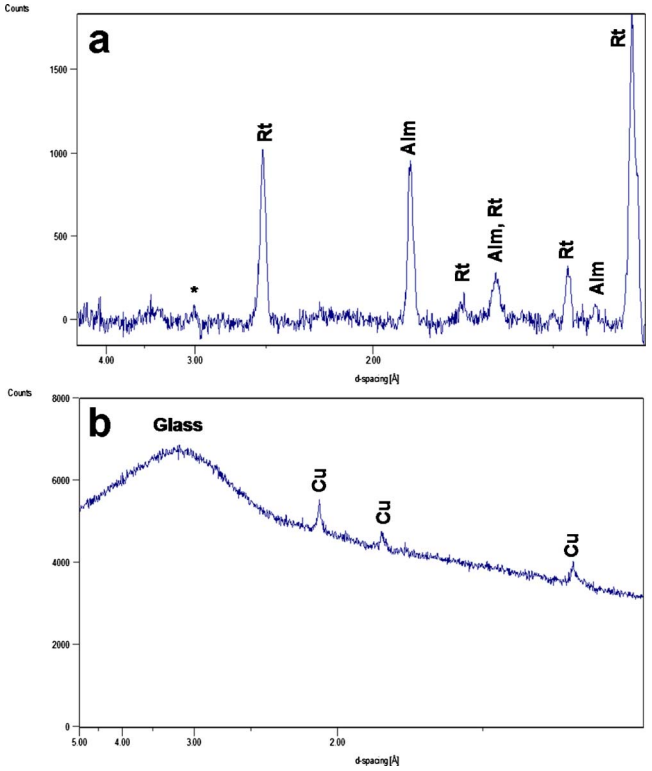

Figure 4. (Color online) Mo LXRPD patterns for (a) gem-165 and (b) gem-340. Labels as in Figure 3.

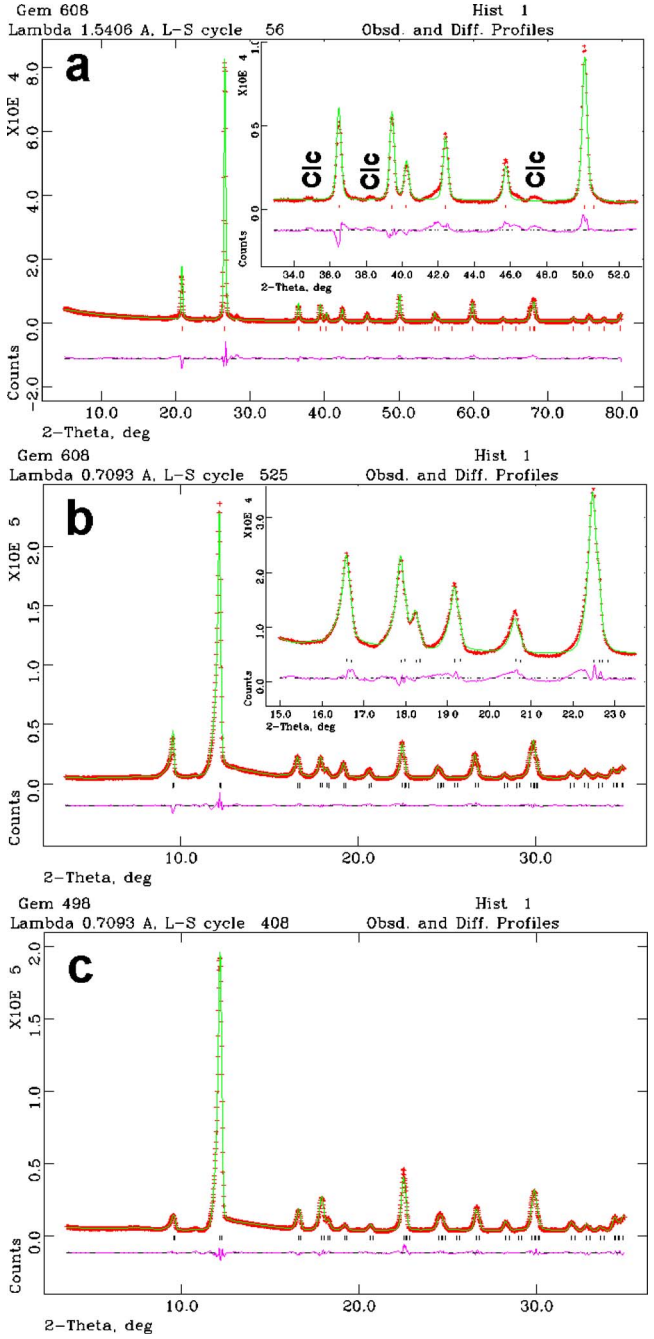

Figure 5. (Color online) Rietveld fitted LXRPD patterns: (a) gem-608 with Cu radiation; (b) gem-608 with Mo radiation; and (c) gem-498 with Mo radiation. The insets in the (a) and (b) panels enlarge a selected region to show the clinochlore diffraction peaks in the Cu pattern and their absence in the Mo pattern.

pattern was collected with strictly monochromatic Cu $K\alpha_1$ radiation. Meanwhile, the Mo pattern was collected with Mo $K\alpha_{1,2}$ radiations. Furthermore, the larger penetration depth of Mo radiation, working in reflection geometry, also results in broader diffraction peaks. Second, it is clear that the recorded diffraction intensities from quartz have the expected values from the standard PDF data as there are many crystallites diffracting in all directions. Third, the crystalline green inclusion has been identified as clinochlore (PDF-01-089-2972) (ICDD, 2004), a member of the chlorite group. Finally, clinochlore diffraction peaks are tiny but evident in the Cu pattern [Figure 5(a)]. However, these peaks are not detected in the Mo pattern [Figure 5(b)]. This can be explained because the inclusion was mainly located at the surface of the gem. In fact, skilled lapidary may cut the gemstones in such a way to expose inclusions on the surface. Taking all together, it is clear that Mo radiation is ideal for the identification/characterization of deep crystalline inclusions and Cu radiation for surface exposed inclusions, as expected from the penetration powers of these radiations. The successful application of the Rietveld method to compact polycrystalline gemstones opens the way for the quantitative phase analysis in suitable samples. For instance, we are already analyzing quartz/moganite mass ratios in compact chalcedonies, and the results will be reported elsewhere. Calcium carbonate quantitative phase analyses for different pearls and related crystalline materials will also be of high interest.

Gemstone 498 (Figure 1) is a quartz showing aventurine effect. The deeply located brown inclusions are highlighted in Figure 2. Figure 5(c) shows the Rietveld fit to Mo LXRPD pattern for this gem. This example has been selected for two reasons. First, the good Rietveld fit supports the use of this methodology for quantitative phase analysis of compact gemstones containing two (or more) microcrystalline phases in mass ratio above a certain limit, still to be established. Second, it is clear that there are no diffraction peaks in addition to those arising from quartz. So, this example highlights the limitations of the technique as it is not always possible to identify the inclusion with the (general) optical setup reported in Sec. II. Microcapillary lens can be used to focus the incident beam on the inclusions in order to collect

https://doi.org/10.1154/1.3552672 Published online by Cambridge University Press

their diffraction pattern. However, the implementation of this methodology is still in progress and it will be reported elsewhere.

IV. CONCLUDING REMARKS AND OUTLOOK

It has been shown that laboratory X-ray powder diffraction is very useful for the identification of crystalline inclusions within gemstones. In particular, Mo radiation patterns are best suited for the identification of deeply buried inclusions. On the other hand, Cu radiation is most adequate for the characterization of surface exposed inclusion. The main merit of this work is the extension of the use of powder diffraction to the bulk gem inclusion characterization without damaging the gem (i.e., without scratching a small portion of the inclusions).

We think that there is a lot of room for further advancement. For example two clear improvements can be carried out. On the one hand, it is possible to use a two-dimensional detector to collect the powder diffraction peaks. In this way, there will be many more (inclusion) crystallites contributing to the diffraction signal. So, the recorded (integrated) intensities will correspond to those gathered in the PDF database, which will help a lot in the identification process when a few types of inclusions coexist within the gemstone. On the other hand, it is also possible to use X-ray microcapillary lens to focus the incident beam. With this optical component, the X-rays can be focused on the inclusions in order to enhance their diffraction signal.

ACKNOWLEDGMENT

The authors thank financial support from research Grant No. FQM-113 from Junta de Andalucía, Spain.

Boiron, M. C., Essarraj, S., Sellier, E., Cathelineau, M., Lespinasse, M., and Poty, B. (**1992**). "Identification of fluid inclusions in relation to their host microstructural domains in quartz by cathodoluminescence," Geochim. Cosmochim. Acta **56**, 175–185.

Ghisoli, C., Caucia, F., and Marinoni, L. (**2010**). "XRPD patterns of opals: A brief review and new results from recent studies," Powder Diffr. **25**, 274–282.

Gübelin, E. and Koivula, J. I. (**1986**). *Photoatlas of Inclusions in Gemstones* (ABC, Zurich), Vol. 1.

Gübelin, E. and Koivula, J. I. (**2005**). *Photoatlas of Inclusions in Gemstones* (Opinio, Basel), Vol. 2.

Gübelin, E. and Koivula, J. I. (**2008**). *Photoatlas of Inclusions in Gemstones* (Opinio, Basel), Vol. 3.

Hatipoglu, M., Tuncer, Y., Kibar, R., Çetin, A., Karali, T., and Can, N. (**2010**). "Thermal properties of gem-quality moganite-rich blue chalcedony," Physica B: Condensed Matter **405**, 4627–4633.

Hughes, R. W. (**1997**). *Ruby and Sapphire* (RWH, Boulder, CO), Chap. 5.

ICDD (**2004**). "Powder Diffraction File," edited by W. F. McClune, International Centre for Diffraction Data, Newtown Square, Pennyslvania.

Jenkins, R. and Snyder, R. L. (**1996**). *Introduction to X-Ray Powder Diffractometry* (Wiley, New York).

Karampelas, S., Hardy, P., and Fritsch, E. (**2010**). "A large hydrogen-rich diamond with a cuboid phantom cloud," Gems. Gemol. **46**, 64–65.

Koivula, J. I. and Chadwick, K. M. (**2008**). "Scapolite with diopside inclusions," Gems. Gemol. **44**, 277–277.

Kretz, R. (**1983**). "Symbols for rock-forming minerals," Am. Mineral. **68**, 277–279.

Langford, J. I. and Louër, D. (**1996**). "Powder diffraction," Rep. Prog. Phys. **59**, 131–234.

Larson, A. C. and von Dreele, R. B. (**2000**). General Structure Analysis System (GSAS), Report LAUR 86-748, Los Alamos National Laboratory, Los Alamos, NM.

Oaki, I. and Imai, H. (**2005**). "The hierarchical architecture of nacre and its mimetic material," Angew. Chem., Int. Ed. **44**, 6571–6575.

Pecharsky, V. and Zavalij, P. (**2008**). *Fundamentals of Powder Diffraction and Structural Characterization of Materials*, 2nd ed. (Springer, Berlin).

Qiao, L., Feng, Q.-L., and Li, Z. (**2007**). "Special vaterite found in freshwater lackluster pearls," Cryst. Growth Des. **7**, 275–279.

Renfro, N. (**2010**). "Hanksite as a gem material," Gems. Gemol. **46**, 60–61.

Rietveld, H. M. (**1969**). "A profile refinement method for nuclear and magnetic structures," J. Appl. Crystallogr. **2**, 65–71.

Tagliani, S. M., Macri, M., Stellino, S., Maras, A., and Serracino, M. (**2010**). "Churrasco quartz' with tourmaline and chamosite inclusions from Brazil," Gems. Gemol. **46**, 63–63.

Tarling, S. E., Barnes, P., and Klinowski, J. (**1988**). "The structure and Si,Al distribution of the ultramarines," Acta Crystallogr., Sect. B: Struct. Sci. **44**, 128–135.

Toby, B. H. (**2001**). "EXPGUI, a graphical user interface for GSAS," J. Appl. Crystallogr. **34**, 210–213.

Toby, B. H. (**2007**). "A new approach for instruction in powder crystallography," Powder Diffr. **22**, 83–84.